Chapter 6
Optimization of MagLev

Jun Xie, Zhengchuan Guo, Chengqian Zhang, and Peng Zhao

6.1 Introduction

The invention of magnetic levitation detection method brings us a potential density measurement and density-based analysis method. The advantages of standard MagLev device have been proved to be (i) of high accuracy, (ii) of high sensitivity, (iii) applicable to smaller objects, such as droplets and powders, (iv) convenient, and (v) low cost.

However, restrictions of standard MagLev still remain. Along with the advantage of low cost brought by the use of permanent magnets comes the restriction of the ability for denser materials. The permanent magnets used in the standard MagLev device can only provide the maximum magnetic flux intensity of 0.475 T at the center on one poles surface. Meanwhile, the maximum concentration of $MnCl_2$ aqueous solution is approximately 5.0 M. Both of the reasons lead to a main restriction that the measurement range of standard MagLev device can be only 0.8–3.0 g/cm^3. Practically, densities of most of the common materials, such as metals, oxides, and salts, are beyond this range.

Therefore, trials on overcoming the problems were carried out by optimizing the MagLev method. This details of the optimizations will be introduced in this chapter.

J. Xie (✉)
College of Mechanical Engineering, Zhejiang University of Technology, Hangzhou, China
e-mail: jxie93@zjut.edu.cn

Z. Guo · C. Zhang · P. Zhao
The State Key Laboratory of Fluid Power and Mechatronic Systems, College of Mechanical Engineering, Zhejiang University, Hangzhou, China

P. Zhao (ed.), *Magnetic Levitation*, https://doi.org/10.1007/978-981-99-8314-8_6

6.2 Enlarging the Measurement Range

Along with the advantage of low cost brought by the use of permanent magnets comes the restriction of the ability for denser materials. The permanent magnets used in the standard MagLev device can only provide the maximum magnetic flux intensity of 0.475 T at the center on one poles surface. Meanwhile, the maximum concentration of $MnCl_2$ aqueous solution is approximately 5.0 M. Both of the reasons lead to a main restriction that the measurement range of standard MagLev device can be only 0.8–3.0 g/cm^3. Practically, densities of most of the common materials, such as metals, oxides, and salts, are beyond this range.

Similar to the effect of the slope in lifting heavy object, the introduction of additional constraint can levitate materials with higher densities with small magnetic force. It is still possible to measure the density of an object by the geometric relationship between the magnetic force and gravity. Two methods are reported to enlarge the measurement range according to this concept.

6.2.1 Tilting the MagLev Device

Tilting the device is the earliest configuration for enlarging the measurement range of MagLev method without increasing the magnetic flux intensity of the magnets [1]. The configuration is based on the standard MagLev device, which has two identical square magnets ($2' \times 2' \times 1'$) with like poles facing each other at a distance of 45 mm. The container filled with paramagnetic solution (typically aqueous $MnCl_2$ or $GdCl_3$) are set vertically to the surface of the magnet. It is easy to predict that a dense object cannot be levitated in standard MagLev device. Hence, when the device is tilted with a certain angle, the dense object would rest at the boundary of the container. In this case, the forces acting on the object are gravity $\overrightarrow{F_g}$, buoyancy $\overrightarrow{F_f}$, magnetic force $\overrightarrow{F_{mag}}$, and the holding force caused by the boundary $\overrightarrow{F_s}$. When the tilting angle is large enough, the most of the gravity would be balanced by the vertical component of $\overrightarrow{F_s}$. Thereby, the object could be pushed away from the bottom of the container by the $\overrightarrow{F_{mag}}$, and reached to an equilibrium position based on its density, as shown in Fig. 6.1. Similarly, the same method can be applied to an object that is much less dense than the solution, which would floats to the top of the container rather than sinking to the bottom. The figure also defines the coordinates for the MagLev frame of reference and laboratory frame of reference. The x- and z-axis are defined as fixed with the device and rotate with the angle θ; the x' - and z'-axis are fixed to the laboratory frame of reference, and do not rotate.

Unlike standard MagLev device, the equilibrium position of the object in tilted device is no longer along with the centerline. Along with the phenomenon is a question: is the equation for $\overrightarrow{F_{mag}}$ along the centerline available or not? To figure out the question, a theoretical analysis was carried out. Previous sections have given the

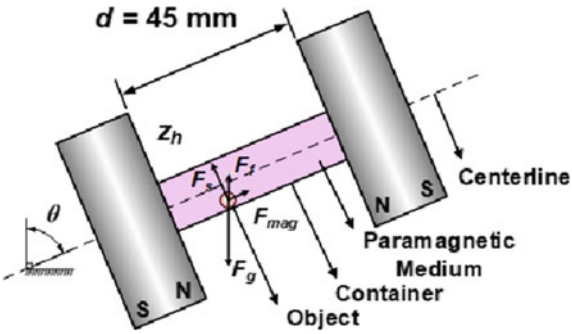

Fig. 6.1 Schematic of tilted MagLev device. Reproduced with permission from Ref. [3]. Copyright 2021 Elsevier

total distribution of the magnetic flux intensity of a standard MagLev device. Based on this distribution, the vertical component (in coordinate for the MagLev frame of reference) $\left(\vec{B}\cdot\vec{\nabla}\right)\vec{B}$ along the centerline and 5 mm away from the centerline is calculated and drawn as curves in Fig. 6.2. It is obvious that the two curves are coincide with each other in the most area. The biggest difference occurs at the surfaces of the two magnets, which is only 0.00027 $T^2\ m^{-1}$ (4.3%). Meanwhile, the previous section also proved that the horizontal component of $\left(\vec{B}\cdot\vec{\nabla}\right)\vec{B}$ can be neglected for it is much smaller than the vertical component. Therefore, the equation for $\overrightarrow{F_{mag}}$ at the boundary 5 mm away from the centerline can be approximately replaced by that along the centerline, which can be expressed as:

$$\overrightarrow{F_{mag}} = \frac{4\Delta\chi B_0^2 V}{\mu_0 d^2}\left(\frac{d}{2} - z\right)\hat{z} \tag{6.1}$$

where, $\Delta\chi = \chi_s - \chi_m$ (unitless) is the difference between the magnetic susceptibilities of object and the medium; $\hat{z}$ is the unit vector of the z-axis; B_0 (T) is the magnetic flux intensity at the surface center of the magnet pole; $\mu_0 = 4\pi \times 10^{-7}$ (N/

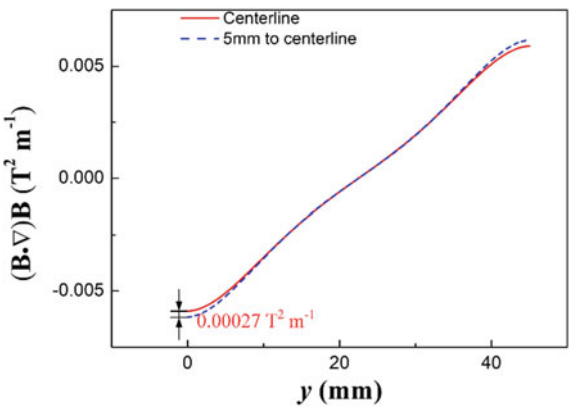

Fig. 6.2 The $\left(\vec{B}\cdot\vec{\nabla}\right)\vec{B}$ along the centerline and 5 mm away from the centerline. Reproduced with permission from Ref. [2]. Copyright 2021 Elsevier

A^2) is the permeability of the free space, and $d = 45$ (mm) is the distance between the two magnets.

In ideal conditions, the sample can be stably held at a position under the balance between the forces $\overrightarrow{F_g}$, $\overrightarrow{F_f}$, ma $\overrightarrow{F_{mag}}$, and $\overrightarrow{F_{bdy}}$,

$$\overrightarrow{F_g} + \overrightarrow{F_f} + \overrightarrow{F_{mag}} + \overrightarrow{F_{bdy}} = 0 \tag{6.2}$$

that is,

$$\left(F_g - F_f\right)\cos\theta = F_{mag} \tag{6.3}$$

According to the expression for each force, the density of the sample ρ_s can be expressed as,

$$\rho_s = \frac{4\Delta\chi B_0^2 V}{\mu_0 g d^2 \cos\theta}\left(\frac{d}{2} - z_h\right) + \rho_m \tag{6.4}$$

where, ρ_m is the density of the medium and z_h is the distance from the sample to the bottom magnet.

Compare Eq. 6.3 with Eq. 5.5, the additional component of the equation is the $\cos\theta$. For the $\cos\theta$ is always less than 1, it is easy to conclude that the measuring range of the device can be directly enlarged. Furthermore, the adjustment of tilting angle θ would result in the change of the measuring range. Theoretically, the measuring range can be infinitely enlarged, as long as the θ is close to 90° enough. In other word, the tilted device has potential to cover the density measurement for all nonmagnetic materials.

However, the ideal condition has a premise that the friction is ignored. In actual environment, the friction plays a very important role in holding the sample stably during the spontaneous levitation of the sample. Therefore, additional processes are considered to avoid the influence of the friction.

Spherical Samples. The rotation of spherical samples can greatly reduce the effect of friction. The friction can be directly ignored under this occasion. During measurement, if the spherical object does not reach to equilibrium position, it would roll and settle at another position (after agitation). If the sphere remained at the same position, regardless of manual agitation, it can be assumed that the sphere reached its equilibrium position. Once this condition was met, the density of the object can be measured using Eq. 6.4. Accordingly, the medium with low viscosity is highly preferred.

Nonspherical Samples. The friction would even prevent a nonspherical object from leaving its initial position. An additional procedure was carried out reduce the effect of the friction: after rotating the container by 180° and then stopping, the sample fell gradually back to the bottom surface of the container. Repeat this procedure several times until the bottom position along the z-axis would no longer change, the state of

the object can be assumed as equilibrated along the z axis. To achieve the overturn of the object's position, high viscosity medium is applied. For instance, 3.00 M $MnCl_2$ solution with aqueous dextran of 35% by weight has the viscosity of approx. 10 Pa s (similar as honey). The highly viscous medium can "carry" the object rotating with the container. Without a viscous liquid, it is hard to overturn the object with the rotation of the container. The object may continue to stay at the bottom regardless of the rate of rotation about the z-axis.

Powders. Similar to nonshperical samples, powders also need to rotate the sample with the container. However, at the scale of powder, fluid resistance increases times larger than that of bulk objects. Therefore, medium with low viscosity is capable for "carry" the powders. On the contrary, highly viscous medium will greatly enlarge the falling time of the powder, which is a waste of time. Unlike single particles, the powders tended to disperse throughout the container during the initial rotations. But the powder will finally converge into a narrow band after enough times of rotation. Additionally, it is also found that rotate the container at a relatively small angle (e.g. rotating 90° instead of 180°), the powder will slide along the surface of the container instead of falling down through the medium. This approach can prevent the dispersion of the particles throughout the container and enable the powder reach to equilibrium position in much less rotations.

The measurement on denser spheres obviously showed the effect on enlarging measurement range, as shown in Fig. 6.3. The materials with large densities, such as Teflon and aluminum (whose densities cannot be measured using the same medium in standard MagLev device), were successfully levitated at their equilibrium positions. Their densities were measured by knowing the z_h and θ. In practical, materials with densities from 0 to over 20 g/cm^3 could all be measured by the method. Table 6.1 showed the results of these materials [1]. The results are in close agreement with those reported by the manufacturer or from other sources. The measurement of same materials in different states (particle and powder) were also well coincidence with each other. In addition, the air was also measured in the tilted device, although the device cannot afford the accurate density measurement of materials with such low density. This indicates that the enlargement of the measurement range is at a large expense of accuracy. The accuracy of the method is two orders of magnitude lower than that of the standard MagLev.

6.2.2 Horizontally Setting the MagLev Device

Horizontally setting the device is another concept to enlarge the measurement range of the device [2]. Similar to tilting the device, this concept introduces an addition constraint to balance a large part of an object's gravity. This constraint is coming from a string attached to the object. The other side of the string is fitted at a certain height. The length of the string L can be adjusted for different occasions. The surface center of the left magnet is set as the origin of coordinates, as shown in Fig. 6.4.

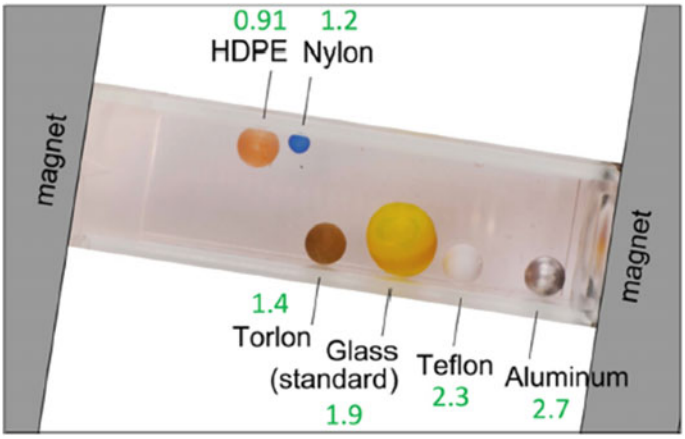

Fig. 6.3 Levitation of denser materials using tilted MagLev device. Reproduced with permission from Ref. [1]. Copyright 2021 American Chemical Society

When the sample is emerged in the paramagnetic medium, it can be pushed away from the surface of the magnet. The three forces the gravity $\vec{F}_g$, the buoyancy $\vec{F}_b$, the magnetic buoyancy caused by the magnetic field $\vec{F}_{mag}$ will get balanced with the additional pulling force from the string $\vec{F}_t$,

$$\vec{F}_g + \vec{F}_b + \vec{F}_{mag} + \vec{F}_t = 0 \tag{6.5}$$

As discussed in previous section, it can be noticed that the $\left(\vec{B} \cdot \vec{\nabla}\right)\vec{B}$ can be assumed as linear, by which the density of the sample can be obtained as Eq. 6.6:

$$\rho_s = \frac{\sqrt{L^2 - d_p^2}}{d_p} \cdot \frac{\Delta\chi}{\mu_0 g}\left(\frac{4B_0^2}{d^2} \cdot d_p - \frac{2B_0^2}{d}\right) + \rho_m \tag{6.6}$$

where L is length of the nylon string. Due to the setting of the coordinates, the distance between the object and the magnet is denoted as d_p instead of z_h.

Several assumptions are made when using this method to measuring density of the denser objects. (i) In this method, the string is assumed as rigid, which means the string will not be stretched or bent during the measuring process. (ii) The $\Delta\chi$ can be approximately replaced by $-\chi_m$, for the magnetic susceptibilities of nonmagnetic materials are always much smaller than that of the medium. (iii) The measuring characteristic along the centerline can be used to measure density throughout the measuring process. It can be noticed that the biggest difference between the $\left(\vec{B} \cdot \vec{\nabla}\right)\vec{B}$ along the centerline and 5 mm away from the centerline occurs at the surface of the two magnet. In addition, the object will derive from the centerline only when it is pushed away from the surface of the magnet. The effect caused by the derivation can

Table 6.1 Densities measurement results of different materials in different states [1]

Material	State	Density (g/cm^3)	
		Known	Measured
High-density polyethylene (HDPE)	Solid (spherical)	0.941	0.95 ± 0.05
Polytetrafluoroethylene (teflon)	Solid (spherical)	2.21	2.2 ± 0.04
Polytetrafluoroethylene (teflon)	Solid (non-spherical)	2.21	2.2 ± 0.05
Glass	Solid (spherical)	2.4–2.8	2.4 ± 0.04
Glass	Powder	2.4–2.8	2.4 ± 0.04
Aluminum	Solid (spherical)	2.7	2.7 ± 0.1
Aluminum	Powder	2.7	2.7 ± 0.04
Silicon nitride	Solid (spherical)	3.32	3.3 ± 0.05
Aluminum oxide	Solid (spherical)	3.88	3.9 ± 0.06
Aluminum oxide	Solid (non-spherical)	3.88	3.9 ± 0.06
Brass	Solid (spherical)	8.53	8.5 ± 0.5
Copper	Solid (non-spherical)	8.96	9.0 ± 0.6
Copper	Powder	8.92	8.8 ± 0.3
Lead	Solid (spherical)	11.2–11.3	11 ± 0.6
Lead	Solid (non-spherical)	11.2–11.3	11 ± 0.6
Mercury	Liquid	13.55	13 ± 0.9
Silicon	Solid (non-spherical)	2.33	2.4 ± 0.04
Diamond	Solid (non-spherical)	3.51	3.6 ± 0.09
Stibnite (Sb_2S_3, mineral)	Solid (non-spherical)	3.88	3.9 ± 0.06
Cerussite ($PbCO_3$, mineral)	Solid (non-spherical)	4.52–4.62	4.5 ± 0.1
Indium	Solid (non-spherical)	7.31	7.3 ± 0.2
Silver	Solid (non-spherical)	10.5	11 ± 0.1
Gold	Solid (non-spherical)	19.3	20 ± 1
Gold	Powder	19.3	19 ± 1
Osmium	Solid (non-spherical)	22.59	23 ± 2
Air	Gas	0.001	0.0 ± 0.04

also be neglected. For example, if the length of the string is 200 mm, the maximum deviation would be less than 1.27 mm, which is much smaller than 5 mm. Therefore, the $\left(\vec{B} \cdot \vec{\nabla}\right)\vec{B}$ along the centerline can be used for density measurements throughout the measuring process.

Practically, the sample cannot be simply considered as a mass point. Thus, the initial position of the sample's centroid cannot coincide with the center of the surface of the magnet. The volume of the sample will affect the measurement range of the device. For instance, assuming that the diameter of the sample is 10 mm and set the L

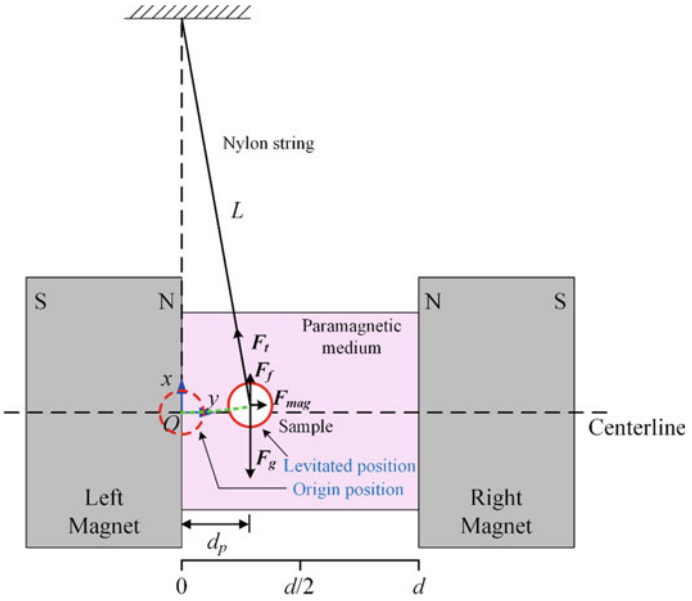

Fig. 6.4 Schematic of horizontally settled MagLev device. Reproduced with permission from Ref. [2]. Copyright 2021 Elsevier

as 200 mm, the measurement range of the device using common solutions are listed in Table 6.2.

Verifications by measuring glass, aluminum, and brass beads, lead to the conclusion that this method has a high accuracy in measuring samples with larger densities, as shown in Fig. 6.5. The measuring results well coincided with the nominal values.

In addition, this method also inherits the advantage of the standard MagLev method that it can measure density without knowing the volume of the sample precisely. This advantage allows the method to quickly obtain the density of samples under some harsh conditions. For instance, the field exploration usually need to know the density of some minerals. Common methods, such as pycnometer and densitometer need the high precision electronic balance, which can only work well

Table 6.2 Parameters for measurement and the measuring range ($L =$ 200 mm)

Standard concentration solutions	Measuring range (g cm^{-3})
1.0 M $MnCl_2$	[1.094, 3.890]
1.5 M $MnCl_2$	[1.148, 5.413]
2.0 M $MnCl_2$	[1.197, 6.931]
2.5 M $MnCl_2$	[1.242, 8.730]
3.0 M $MnCl_2$	[1.292, 9.949]

Reproduced with permission from Ref. [2]. Copyright 2021 Elsevier

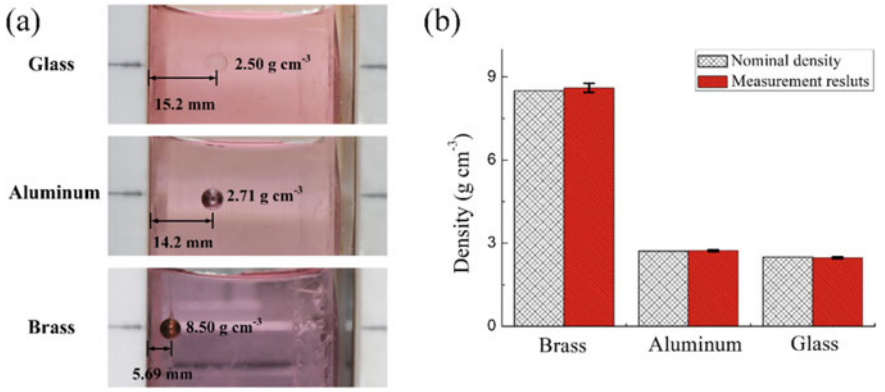

Fig. 6.5 Verifications by measuring density of glass, aluminum, and brass beads. **a** Levitation results in horizontally settled device. **b** The calculated results of glass, aluminum, and brass beads. Reproduced with permission from Ref. [2]. Copyright 2021 Elsevier

in laboratory conditions. The MagLev method provides a potential solution for rapid measurement of mineral particles in outdoor occasions.

Trials on different minerals were carried out (Fig. 6.6). Their measurement results are listed in Table 6.3. It can be noticed that the MagLev method is capable for substituting the common methods. The advantage of portability and energy-free additionally make the method be more suitable for outdoors' occasions over common methods.

However, this method also has relatively more restrictions compared with tilted MagLev device. The most important difference is that the device can only measure solid particles. The measuring process need to adhere the sample with the string.

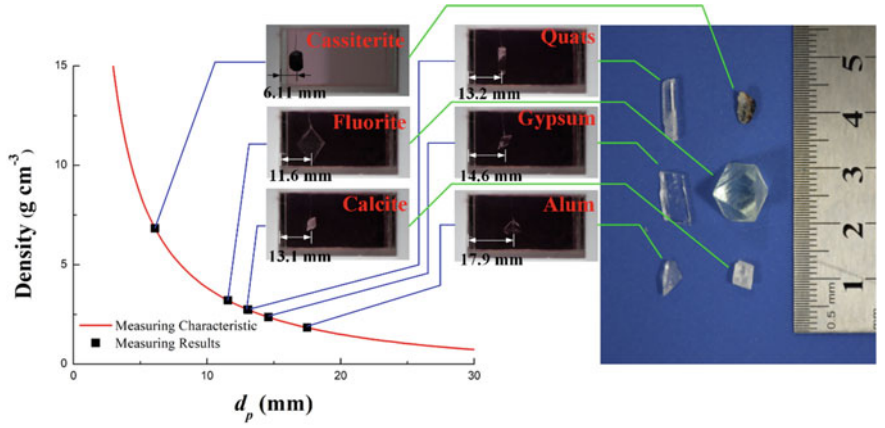

Fig. 6.6 Density measurement of different mineral particles. Reproduced with permission from Ref. [2]. Copyright 2021 Elsevier

Table 6.3 Density measurement results of different minerals [2]

Single particle							Multiple particles	
Minerals	Levitation height (mm)	Calculated results (g cm^{-3})	Average results (g cm^{-3})	Mean square error (g cm^{-3})	Pycnometer results (g cm^{-3})	Densitometer results (g cm^{-3})	Pycnometer results (g cm^{-3})	Densitometer results (g cm^{-3})
Alum	17.6	1.818	1.828	0.011	1.655 $\pm$ 0.151	1.858	1.826 $\pm$ 0.006	1.829
	17.4	1.839						
	17.4	1.837						
	17.5	1.830						
	17.6	1.816						
Gypsum	14.5	2.369	2.347	0.025	2.102 $\pm$ 0.076	2.386	2.324 $\pm$ 0.012	2.351
	14.7	2.334						
	14.7	2.322						
	14.5	2.377						
	14.7	2.331						
Quartz	13.7	2.560	2.573	0.031	2.499 $\pm$ 0.136	2.598	2.578 $\pm$ 0.012	2.580
	13.5	2.609						
	13.6	2.584						
	13.6	2.584						
	13.8	2.528						
Calcite	13.1	2.702	2.727	0.029	2.428 $\pm$ 0.292	2.673	2.722 $\pm$ 0.014	2.744
	13.0	2.735						
	12.9	2.774						
	13.1	2.707						
	13.1	2.717						

(continued)

Table 6.3 (continued)

Single particle							Multiple particles	
Minerals	Levitation height (mm)	Calculated results (g cm^{-3})	Average results (g cm^{-3})	Mean square error (g cm^{-3})	Pycnometer results (g cm^{-3})	Densitometer results (g cm^{-3})	Pycnometer results (g cm^{-3})	Densitometer results (g cm^{-3})
Fluorite	11.5	3.187	3.182	0.012	3.161 $\pm$ 0.132	3.192	3.180 $\pm$ 0.008	3.197
	11.6	3.174						
	11.6	3.166						
	11.5	3.188						
	11.5	3.195						
Barite	8.9	4.380	4.317	0.073	4.412 $\pm$ 0.238	4.381	4.310 $\pm$ 0.023	4.342
	9.0	4.320						
	9.2	4.193						
	8.9	4.354						
	9.0	4.337						
Cassiterite	6.2	6.650	6.742	0.072	6.790 $\pm$ 0.331	7.009	6.754 $\pm$ 0.011	6.747
	6.1	6.776						
	6.1	6.754						
	6.1	6.695						
	6.0	6.836						

Thus, this device is not capable for gas, powder, and liquid samples. In addition, the constraint from the string can only prevent the sample from sinking to the bottom of the container. This means the horizontally set device also cannot measure the sample with density lower than the medium.

6.3 Improving the Sensitivity

Equation 5.6 was deduced to measure the density of an object levitated along the centerline of a MagLev device. Higher sensitivity of a MagLev device means it can distinguish small differences in ρ_s by an obvious change of z_h. Thus, the sensitivity of a device can be defined as its ability to distinguish the difference in density $\Delta\rho_s$ caused by the change in levitation Δz_h. It is known that $\Delta\rho_s = f'(z_h)\Delta z_h$. Then we defined the sensitivity using Eq. 6.7.

$$S(z_h) = \left| \frac{1}{f'(z_h)} \right| \tag{6.7}$$

Here, $S(z_h)$ denotes the sensitivity of the device. Larger $S(z_h)$ equals higher sensitivity. Note that $S(z_h)$ could be influenced by χ_m, the structure of the device (d), the magnets used in the device, and the position of the sample (z_h). This study emphasised the influence of d. The comparisons in each section were conducted using a medium with the same $MnCl_2$ concentrations. The magnets were the same in all of the experiments.

6.3.1 Enlarging the Distance Between the Magnets

Although standard MagLev device has high accuracy and sensitivity in measuring density, it still has place to be improved. It can be easily predicted that enlarging the distance between the magnets is a potential way to enlarge the sensitivity of the device. However, the relationship between the density and levitation height become no longer linear. Hence, further theoretical analysis should be discussed.

For the improvement is based on the standard MagLev device, the magnets are chosen as N45 magnets with the size of 50 mm × 50 mm × 25 mm. Based on the magnets, the performance of the device under different d is further plotted in Fig. 6.7 [3]. As mentioned above, the stable levitation along the centreline is required to guarantee the accurate measurement. According to the performance of the device, although the calculation curve of device with $d = 70$ mm shows the highest sensitivity above the other two curves (Fig. 6.7d), it cannot ensure levitating the sample steadily along the centreline (Fig. 6.7c). The device with $d = 60$ mm has a relatively higher sensitivity and a larger manipulation space than those of the standard MagLev device (Fig. 6.7b, d).

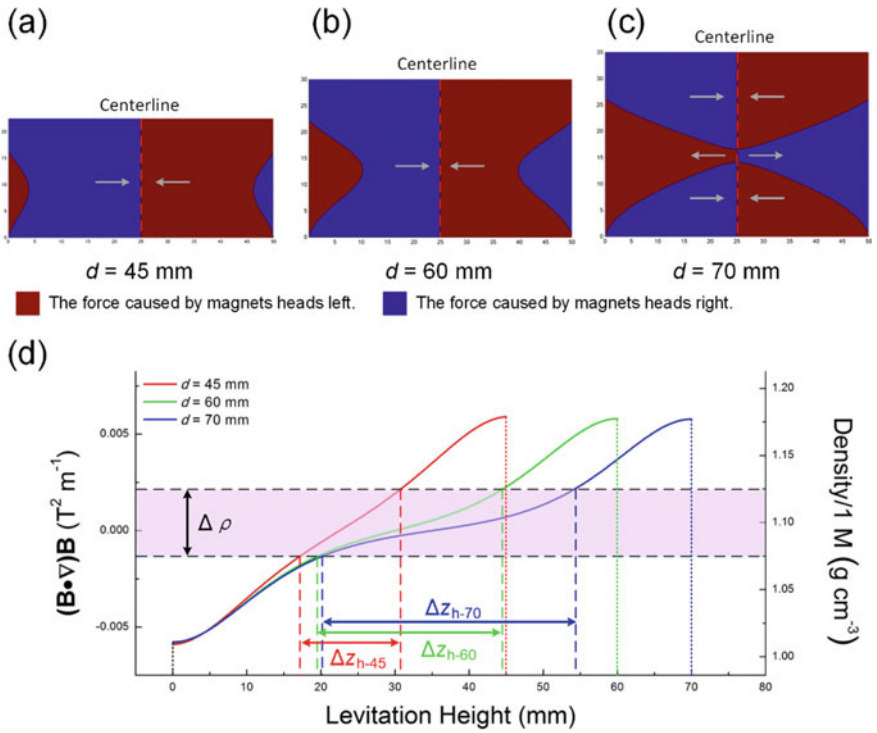

Fig. 6.7 **a**–**c** Calculation results of device with $d = 45$ mm, $d = 60$ mm, and $d = 70$ mm, respectively. The magnets are set as the same in these calculations. The magnets are N45 of 50 mm × 50 mm × 25 mm. For the symmetry of the device, each figure only shows bottom half of the calculation in the space between two magnets. **d** Calculation results of $\left(\vec{B} \cdot \vec{\nabla}\right)\vec{B}$ along the centreline under different *d*. Reproduced with permission from Ref. [3]. Copyright 2021 Elsevier

According to the aforementioned density measurement calculation, the expression for the standard MagLev device is a first-order expression. Therefore, for a given paramagnetic medium, $S(z_h)$ of the standard MagLev device is a constant value. On the other hand, $S(z_h)$ of the device with $d = 60$ mm can be obtained as a second-order expression (Eq. 6.8) [4]. For the same paramagnetic medium (2.0 M $MnCl_2$ aqueous solution, for example), $S(z_h)_{60}$ (from $z_h = 12.71$ to 47.29 mm) is larger than $S(z_h)_{45}$ in most areas. It can be easily observed in Fig. 6.7, for the slope of the expression of the device with $d = 60$ mm is obviously smaller than that of the device with $d = 45$ mm.

$$\Delta\rho_s = \left(-50.055 + 2.748x - 4.602 \times 10^{-2}x^2\right)\chi_m \cdot \Delta z_h = \frac{1}{S(z_h)_{60}}\Delta z_h \quad (6.8)$$

A series of experiments on standard density beads can reveal the effect of high sensitivity. The five beads with densities of 1.1000, 1.1500, 1.2000, 1.2500 g cm^{-3},

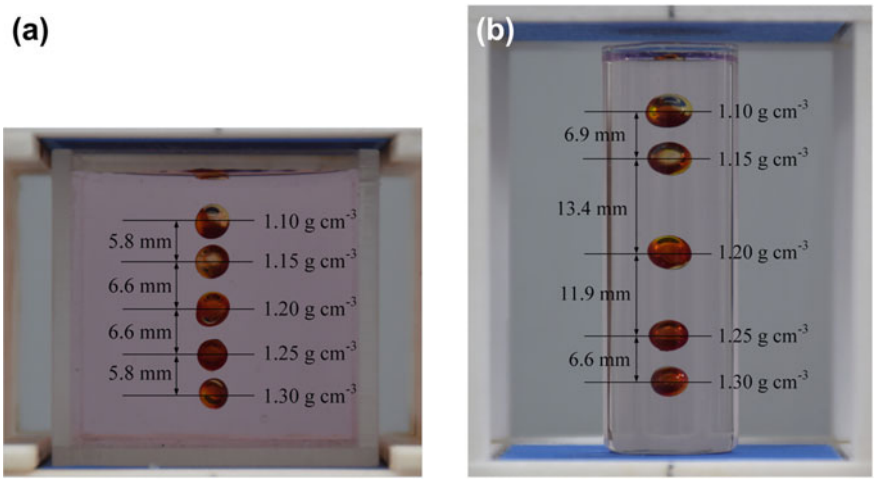

Fig. 6.8 Levitation of standard density beads in **a** standard MagLev device, and **b** high-sensitivity MagLev device device. Reproduced with permission from Ref. [4]. Copyright 2018 Elsevier

and 1.3000 g cm^{-3} were levitated simultaneously, as shown in Fig. 6.8. The gap of z_h between the adjacent beads in the device with $d = 60$ mm was larger than in the standard MagLev Device. Moreover, in the device with $d = 60$ mm, the levitations near the middle plate between the magnets have larger gap than in other areas. This area (Fig. 6.8b, z_h from 20 to 40 mm) is called a high sensitivity area. The $S(z_h)_{60}$ in this area reached 204 and 305 mm cm^3 g^{-1}, which is 1.67–2.50 times larger than that of the standard MagLev device.

High sensitivity enabled the devices to tolerate larger disturbances in z_h caused by environmental or other random factors. Small differences in z_h did not cause distinct deviation in measuring ρ_s. The devices were also better at measuring samples whose force centres were difficult to determine. Thus, enhancing sensitivity provided higher accuracy. Moreover, devices with higher sensitivity can distinguish miniscule differences in densities. Thus, such devices can be used to separate objects with similar densities.

For example, thermoplastic urethane (TPU, BASF 1190A) and polylactic acid (PLA, NatureWorks 3001D) have very similar densities (1.112 g cm^{-3} vs. 1.242 g cm^{-3}). Although single particles can be distinguished by the standard MagLev device (by a 7.54 mm interval between their levitation heights), the device is insufficient to separate multiple particles, as shown in Fig. 6.9a, b. It can be observed that the clusters of two materials had an obvious interference (red circle in Fig. 6.9b) that the two materials were not completely separated. Changing the device of high sensitivity, the mixed particles were separated again in the same medium (Fig. 6.9c). As predicted above, the interval between their respective levitation heights increased 70% (12.09 mm). $S(z_h)_{60}$ in this interval ranged from 293 to 304 mm cm^3 g^{-1}, which

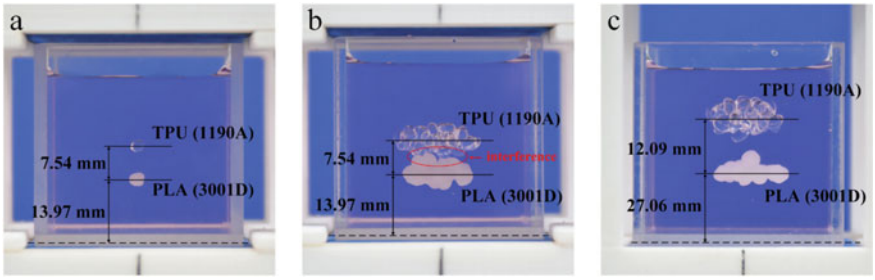

Fig. 6.9 Separating experiments involving TPU (1190A) and PLA (3001D). **a** Separation of two single particles. **b** Separation of two masses of samples in the device with $d = 45$ mm. **c** Separation of two masses of samples in the device with $d = 60$ mm. Reproduced with permission from Ref. [4]. Copyright 2021 Elsevier

is much larger than $S(z_h)_{45}$ (122 mm cm^3 g^{-1}). The two materials become no longer adhere to each other. Hence, the two materials were completely separated.

In addition, high sensitivity not only means the MagLev device can distinguish minute differences among varying samples, but also suggests it is sensitive to defective prats. The defect interior a part will cause the misalignment of the centre of mass and the geometric centroid. When the difference between the moments caused by the magnetic force and the gravity balances each other, the sample reaches its equilibrium position. Higher sensitivity means the magnetic force changes more slowly in the vertical direction. Thus, the sample's equilibrium position deflects a larger angle from the horizontal position. The effect of high sensitivity can be revealed in the test of polycarbonate (PC) washers as shown in Fig. 6.10. For the washers have the symmetrical structure, the levitation position of the homogeneous washer should be horizontal (Fig. 6.10d, g). On the contrary, the defective washers would deflect from the horizontal position. Results in standard MagLev device verified the prediction, as shown in Fig. 6.10d–f: The heterogeneous washer was levitated horizontally. The angle of the washer with small interior bubbles was 6.9°. The washer with larger interior bubbles deflected a larger angle of 27.1°.

Remain the experimental condition unchanged, the washers were levitated in high sensitivity device. Coincidently, the levitation heights of the washers were in the range of the high sensitivity area (from 32.29 to 32.60 mm). $S(z_h)_{60}$ at this height was 2.4 times greater than $S(z_h)_{45}$. Due to the substantial increase in $S(z_h)$, the defective washers all deflected larger angles (15.0° vs. 6.9° and 27.1° vs. 64.8°, see Fig. 6.10h, i). The results indicate that: (i) the levitation position of defective samples deflected from that of the homogeneous sample and (ii) enhancing the device's sensitivity increases the deflect angle of the defective sample. Therefore, the device with higher sensitivity is more appropriate for samples with minute defects.

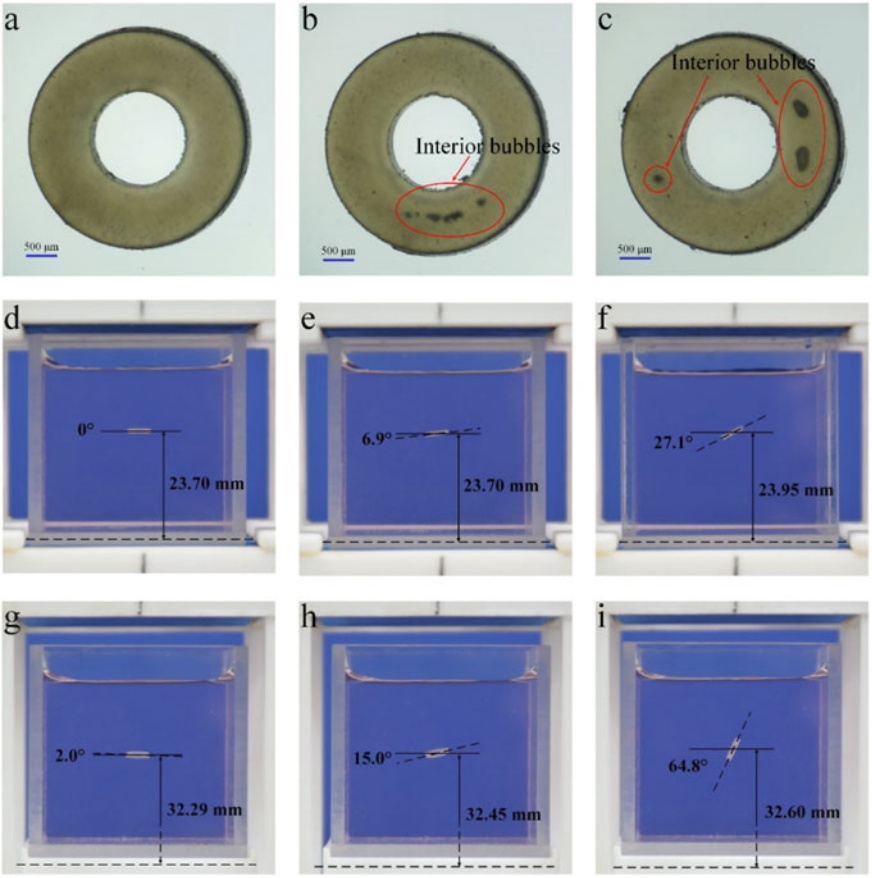

Fig. 6.10 **a** Micrographs of the homogeneous washer. **b** Micrographs of the washer with small interior bubbles. **c** Micrographs of the washer with large interior bubbles. **d–f** Levitation positions of the washers in the device with $d = 45$ mm. **g–i** Levitation positions of the washers in the device with $d = 60$ mm. Reproduced with permission from Ref. [4]. Copyright 2021 Elsevier

6.3.2 Enhancing Sensitivity by Introducing Additional Centrifugal

In standard MagLev device, the objects are levitated along the centerline, which is vertical to the ground. Some researchers conceived a rotating method, which can levitate objects along an oblique line without tilting the device [5]. The testing platform is designed as Fig. 6.11a. Two additional magnets were added to the MagLev device for balancing the centrifugal force. Each pair of magnets were arranged with like poles facing each other. Objects with close densities may cluster in the levitation for the lack of sensitivity, as shown in Fig. 6.11b. The rotation of the platform gives the sample an additional centrifugal force, which pushes the sample away from the

centerline of the MagLev device. The magnetic force generated by the horizontal pair of magnets will prevent the sample from leaving the centerline. When the two forces on horizontal direction meet the balance, the sample reaches to a new equilibrium position. For the centrifugal force can be expressed as Eq. 6.9, the equilibrium conditions of the sample can be updated as Eqs. 6.10 and 6.11.

$$F_c = m_s\omega^2(d_e - x) = \rho_s V\omega^2(d_e - x) \tag{6.9}$$

$$F_x = \frac{\Delta\chi}{\mu_0}\left|\left(\vec{B}\cdot\vec{\nabla}\right)\vec{B}\right|_x V - (\rho_s - \rho_m)\omega^2(d_e - x)V = 0 \tag{6.10}$$

$$F_z = \frac{\Delta\chi}{\mu_0}\left|\left(\vec{B}\cdot\vec{\nabla}\right)\vec{B}\right|_z V - (\rho_s - \rho_m)gV = 0 \tag{6.11}$$

where, ω is the rotating speed of the plate and d_e is the eccentric distance (as shown in Fig. 6.11a).

As can be easily noticed, the density of the object can not only be calculated by its levitation height, but also can be a function of d_x:

$$\rho_s = \frac{\Delta\chi}{\mu_0\omega^2(d_e - x)}\left(\vec{B}\cdot\vec{\nabla}\right)B_x + \rho_m \tag{6.12}$$

The slice of the distribution of magnetic field in the x–z plane on the centerline is shown in Fig. 6.12. The changes of B_x and $\left(\vec{B}\cdot\vec{\nabla}\right)B_x$ for varying x and z are shown in Fig. 6.12b, c. It can be observed that in certain areas ($x \in [-10.0\,\text{mm}, 10.0\,\text{mm}]$ and $z \in [-10.0\,\text{mm}, 10.0\,\text{mm}]$), these two values vary linearly with x, which means

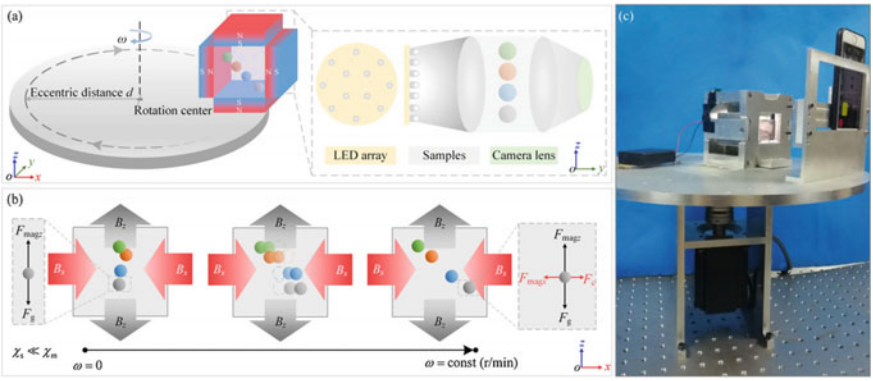

Fig. 6.11 The centrifugal magnetic levitation approach for density measurement. **a** Schematic of the measurement system. **b** Illustration of the dynamic migration process of the levitation positions under the combined effect of magnetic forces, gravity and centrifugal force. **c** Prototype platform for the density measurement using the centrifugal magnetic levitation approach. Reproduced with permission from Ref. [5]. Copyright 2021 Elsevier

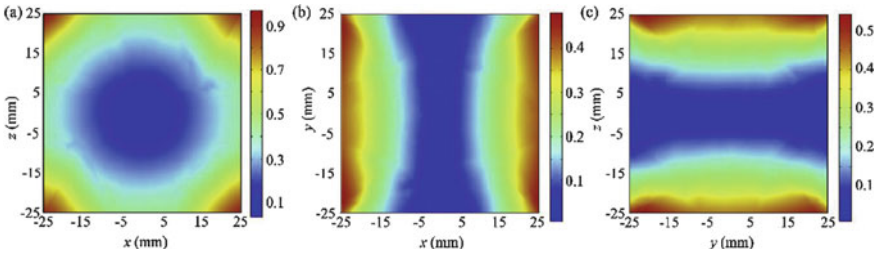

Fig. 6.12 3D simulation model of the magnetic field distribution. **a** The x–z section at y = 0. **b** The x–y section at z = 0. **c** The y–z section at x = 0. The magnetic field is symmetric with the center at the plane of x–z, x–y and y–z. Reproduced with permission from Ref. [5]. Copyright 2021 Elsevier

the relationship between ρ_s and x can also be approximately expressed as a linear function:

$$\rho_s = \frac{\Delta\chi}{\mu_0\omega^2}\frac{x}{(d_e - x)}B_x'^2 + \rho_m \tag{6.13}$$

According to the function, a larger eccentric distance d_e and a higher rotation rate ω will provide larger centrifugal force. This can result in a larger deviation of an object from centerline of the device. Under this condition, objects with similar densities will have larger intervals between each other. In other words, the measurement has a larger sensitivity.

The series of experiments on standard density beads validates the conclusion, as shown in Fig. 6.13. In the figure, the grey curves in Fig. 6.13 are positions of each constant ρ_s vary with the change of ω, while the blue curves represent levitation position as a function of density ρ_s under constant rotation speed. The beads with the density of 1.06, 1.09, and 1.11 g/cm^3 were levitated in the 0.8 M $MnCl_2$ aqueous solution. The device was driven to rotate at the d_e of 30 mm and 60 mm. The rotation speeds are ranging from 50 to 160 r/min with the interval of 5 r/min. The points of the results well landed on their theoretical curves. As the result, the beads spread apart more obviously with larger eccentric distance and higher rotation speed. The highest resolution of minute differences in density was calculated to be 0.003 g/cm^3 in these results. In fact, continue to increase the eccentric distance and rotation speed within a reasonable can further increase the sensitivity during measurement.

As discussed above, the most direct effect of high sensitivity is that the device can separate objects with similar densities more obviously. The example given in the research of the rotating device fully demonstrated this effect. The experiment is a levitation of PMMA particles with different interior bubbles. These interior bubbles cause the differences of densities among the particles (Fig. 6.14a). For the lack of sensitivity, the little differences can not lead to the total separation of each particle in static device (Fig. 6.14b). When rotating the device at a speed of 140 r/min, the particles arranged on a sloping curve, as shown in Fig. 6.14c. Therefore, the particles got obviously separated. It is also worth noting that, the sensitivity of the rotating

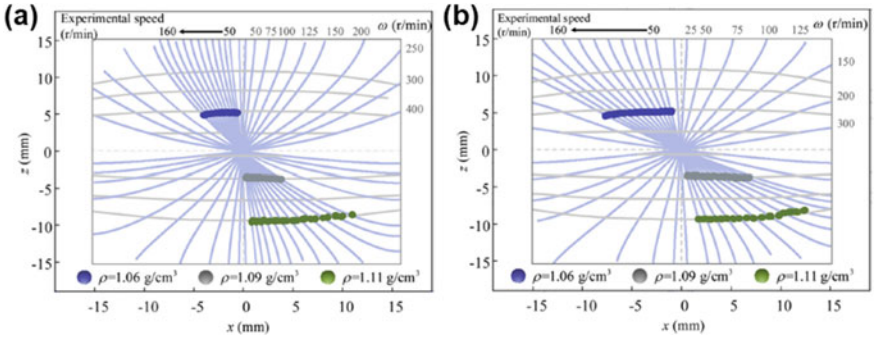

Fig. 6.13 Effect of the eccentric distance on the spatial levitation positions as a function of rotating speeds. Three standardized beads with densities of 1.06 g/cm^3 (blue), 1.09 g/cm^3 (grey) and 1.11 g/cm^3 (green) were levitated in a 0.8 M $MnCl_2$ aqueous solution with different eccentric distances: **a** d = 30 mm. **b** d = 60 mm. Reproduced with permission from Ref. [5]. Copyright 2021 Elsevier

device does not remain a constant value. It reaches approximate two times larger than that of the static device when levitating denser objects.

In general, the MagLev device has a potential structure that simple improvement can improve its sensitivity without sacrificing the measuring range. The improvement of sensitivity is a promising method for distinguishing and separating similar densities.

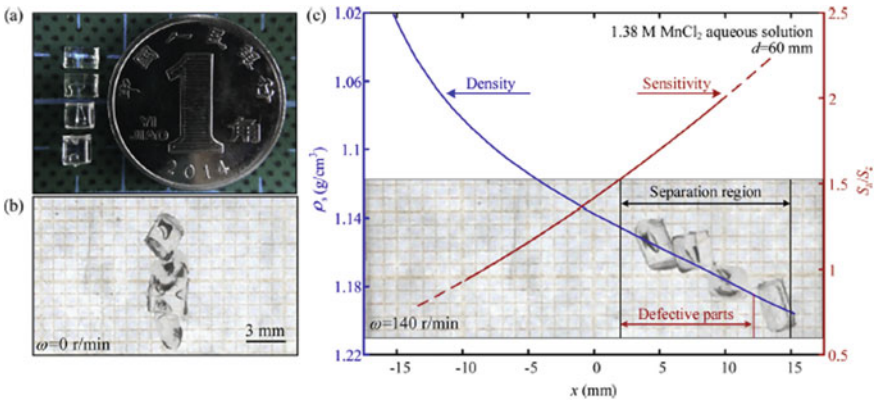

Fig. 6.14 Separation of PMMA particles with internal defects. **a** Image of four small transparent PMMA particles (millimeter-sized) and one coin with a diameter of 19 mm. **b** Image of the clustered particles along the centerline of the device in an aqueous solution of 1.38 M $MnCl_2$ when the MagLev device was static. The scale bar is 3 mm. **c** Separation of particles in the same batch when the rotating speed was 140 r/min with the eccentric distance of 60 mm. Reproduced with permission from Ref. [5]. Copyright 2021 Elsevier

6.4 Changing the Magnets

Changing magnets is a way that researchers tried to meet the requirements of different fields. The research have proved that except for the squared magnets, magnets with other shapes can also achieve stable levitation of object, as long as the magnets have same poles facing each other. The following parts will introduce the achievements on MagLev device using magnets with different shapes in specific application scenarios.

6.4.1 Using Ring Magnets

As we can find in common markets, round magnets are good substitutes for the square magnets. In fact, using round magnets is similar as using square magnets. Therefore, almost no research focused on these devices. However, using ring magnets brought many interesting characters into the MagLev Device.

The improvement began with the direct change of the square magnets, which is given a name of "axial MagLev device" [6]. All the characteristics that standard MagLev device has can be observed in the axial MagLev device: (i) the diamagnetic object can be stably levitated on the centerline; (ii) the distribution of magnetic field is approximately linear along the centerline. Of course, these characteristics also require the certain distance between the magnets. For instance, the inner diameter (r)/outer diameter (R)/height (h)/distance between magnets (d) = 1:3:1:0.6 can fully satisfies the condition. Equations 5.8–5.11 can be copied for the axial MagLev device. Clearly, the hole of the ring magnet has significant effect on the distribution of the magnetic field, as well as the B_0. Hence, to maintain the linear distribution of magnetic field, the distance between the magnets is much smaller than that of the comparable standard MagLev device (16 mm vs. 45 mm). Instead, the narrow space between magnets multiplies the gradient of the magnetic field (see Eqs. 5.10 and 5.11). Consequently, the measuring range gets enlarged that it can measure lighter/denser materials. As shown in Fig. 6.15, air bubble (0.001 g/cm^3) and zirconium silicate (3.73 g/cm^3) can be levitated and measured, which is impossible for standard MagLev device (measuring range from 0.8 to 3.0 g/cm^3).

Accordingly, enlarging the distance between the magnets makes the distribution of magnetic field along the centerline no longer linear. The phenomenon is also related to the shape of the ring magnets (e.g. inner diameter/outer diameter and the height of the magnet). This change can be modeled by the theoretical analysis. According to the model, the density measurement can be achieved by the device using any kind of ring magnets. Two pairs of magnets (H20 magnets: r × R × h = 20 × 30 × 20 mm, B_0 = 1.23 T; H10 magnets: r × R × h = 12.5 × 25 × 10 mm, B_0 = 0.88 T) are calculated as examples as shown in Fig. 6.16. When the distance between the magnets remains 20 mm, the two pairs of magnets can both stably levitate the objects. The relationships between the density and levitation height are monotonical, although the relationship for H20 magnets is much more linear. This means the density can

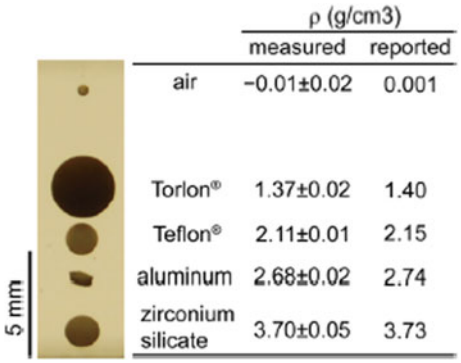

Fig. 6.15 Levitation and density measurement of objects using axial MagLev device. Reproduced with permission from Ref. [6]. Copyright 2021 American Chemical Society

be obtained directly by knowing the levitation height of an object. With the increase of the distance between the H20 magnets, the linearity between the density and the levitation height no longer exists. Similar to the enhancement of the sensitivity of standard MagLev device, the curvature of the relationship curve becomes larger, which brings higher sensitivity and an area of ultra-high sensitivity.

An interesting phenomenon occurs along with the continuous increase of the distance between the magnets. As mentioned in previous sections, the MagLev device using square magnets cannot levitate objects stably with a large distance between the magnets. Enlarging the distance between the magnets in Axial MagLev device leads to a total different result [7]. Yet the equilibrium position for a levitated object is no longer along the centerline, a bell-shaped area for stable levitation is generated, as shown in Fig. 6.17. The three dimensional levitation is also an approach to obtain higher sensitivity. Particularly, the bell-shaped area allows the objects have choice for different equilibrium positions. Hence, the hamper from each other can be drastically reduced, which is an advantage in measuring multiple samples. In fact, the increase of the sensitivity is not the most valuable contribution of bell-shaped area. Reasonable

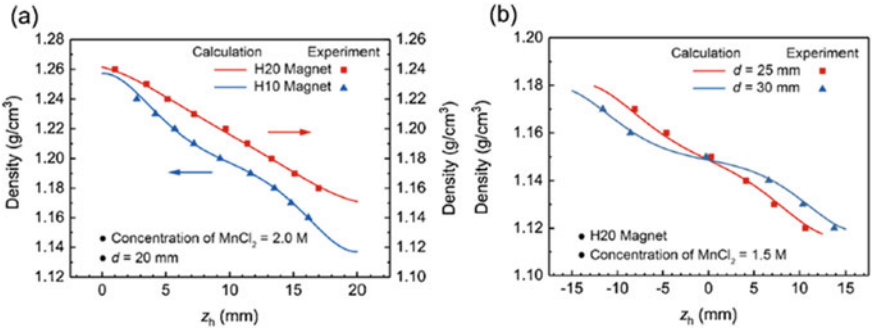

Fig. 6.16 Relationship between density and levitation height using different pair of magnets. Reproduced with permission from Ref. [8]. Copyright 2021 Elsevier

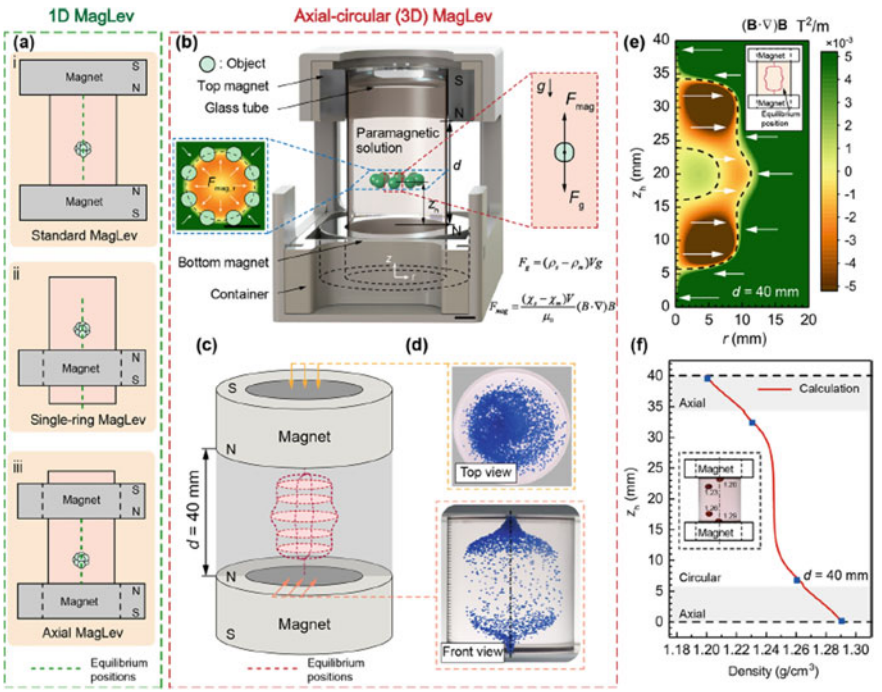

Fig. 6.17 Three dimensional (3D) levitation using ring magnets. **a** Schematic of 1D MagLev. **b** Schematic of 3D MagLev. **c** Bell shape area for stable levitation. **d** The levitation of particles spread over the bell shape area. **e** Theoretical calculation of magnetic force near the bell shape area. **f** Relationship between levitation height and density. Reproduced with permission from Ref. [7]. Copyright 2021 American Chemical Society

use of this area can further realize the manipulation of particles. This approach will be introduced in the following parts.

Beyond common prediction, further increase the distance between the ring magnets is still meaningful. The equilibrium positions of the objects come back to the centerline when the *d* reaches to 105 mm. Under this condition, the sensitivity of the device reach to a very high level (140 times larger). It is not a good choice to use the device to measure density of a sample, for the preparation of the medium should be more precise. The parameters, such as density and magnetic susceptibility, are required to be obtained accurately. This will make the MagLev lose its advantage of convenience. However, the high sensitivity is very useful for separation of sample with very similar densities, or the distinguish of unknown substances.

The device also has advantages over standard MagLev device of the ability to manipulate and observe the sample from top side [8]. A schematic of the combination of MagLev and ultrasonic is shown in Fig. 6.18. The levitation of object not only can measure the density and evaluate the quality of the sample, but also acts as a fixture. Therefore, the sample can be further detected by the ultrasonic with a certain

posture. For example, the levitation postures of the plates shown in Fig. 6.18b can be easily predicted as horizontal. Therefore, it is easy for ultrasonic to measure the height of the plates. In fact, the MagLev is a kind of non-contact levitation. Thus, it can prevent some disturbance from fixture, which makes the additional testing techniques test samples with complex structures. However, the levitation posture for a certain sample is determined. The sample may also rotate during the levitation. These may affect the testing results.

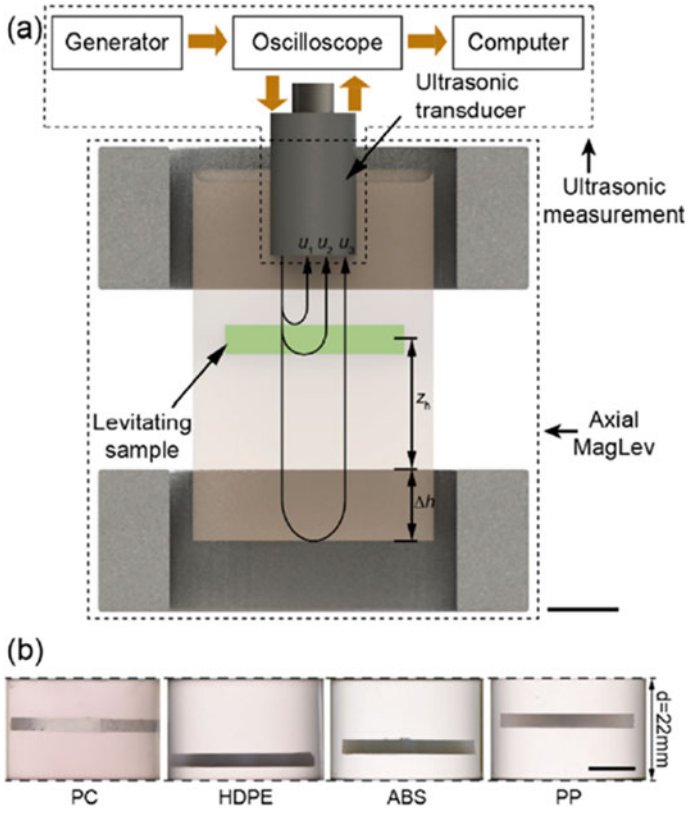

Fig. 6.18 The scheme of method combining the axial MagLev and the ultrasonic measurement. **a** A schematic representation of the measurement device. The ultrasonic transducer is fixed coaxially with the ring magnets. **b** Experimental photographs for various materials using device with d = 22 mm. The scale bars are 10 mm in length. Reproduced with permission from Ref. [8]. Copyright 2021 Elsevier

6.4.2 Using Magnet Arrays

One of the most prominent advantages of MagLev device is its portability. It is benefited from the market-available permanent magnets. In addition, the price of the magnets is relatively cheaper. Usually, the magnets used in standard MagLev device have the size of $2'' \times 2'' \times 1''$, which cost approximately $15 per piece. This kind of NdFeB magnets can generate a magnetic field has the maximum $B_0 = 0.475$T, which can afford the levitation of common materials, as introduced in previous sections. However, it disadvantage is also obvious that the size of magnet limits the maximum size of the sample: the standard MagLev can levitate sample with the diameter of 10 mm, while can only measure sample with maximum thickness of only 3–4 mm. Although using large magnets is a possible way, it lack the feasibility for the following two reasons. (i) The cost of the mold for manufacturing larges size magnets is too large. Meanwhile, the market of the large magnets cannot make manufacturers profitable. Thus, the manufacturer tend not to provide the large magnets. (ii) The magnetization direction cannot be ensured when magnetizing large magnets. This will cause the magnetic field of MagLev device is different from the prediction and then affect the levitation.

Therefore, special arrangements of a group of magnets is a possible way to solve the problem. Halbach Array is a near-ideal structure that can generate the strongest magnetic field with the least amount of magnets. It is conceived by Klaus Halbach in 1979, when he was experimenting with electron acceleration. However, the distribution of Halbach array is a bit more complex. Although it can generate a large magnetic field with a large gradient, it requires in depth analysis to figure out a proper structure for stable magnetic levitation.

In fact, that if we arrange magnets close together with the same direction of the poles, the magnet array can be assumed as a whole magnet. According to the Ampere molecular circulation hypothesis, the surface equivalent current of each magnet can be counteracted by their near neighbor magnets. Hence, the equivalent current of outermost surface of the magnet arrays is connected in series, which is the same as a whole magnet. Predictably, this arrangement of the magnets definitely causes large repulsive force from adjacent magnets. This requires additional structure to constrain the magnets. For small magnets, an iron plate with special fixtures can achieve the purpose. When facing the large magnets, the fix with bolts is highly required.

It has been proved that using magnet arrays to construct MagLev devices is feasible [9]. Eight identical N35 magnets with the size of 20 * 20 * 10 mm are used to replace the integrated N35 magnets with the size of 40 * 40 * 20 mm. The simulations of the magnetic fields are shown in Fig. 6.19. Obviously, the results are almost the same. This directly results in the similarity of MagLev devices using magnet arrays and integrated magnets. In Fig. 6.19c, d, the simulation of $\left(\vec{B} \cdot \vec{\nabla}\right)\vec{B}$ on horizontal direction indicates the device can afford the stable levitation along the centerline (similar results were discussed in Chap. 5. Thus, the basic function, density measurement, can be realized.

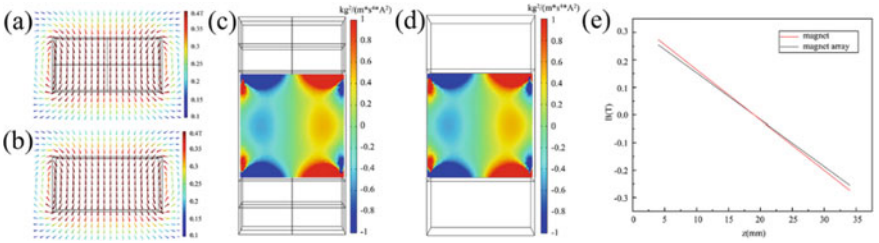

Fig. 6.19 Schematic diagram of the equivalent currents of the magnets. **a** The distribution of magnetic flux intensity of magnet array. **b** The distribution of magnetic flux intensity of single square magnet. **c** The distribution of the gradient magnetic flux intensity of standard MagLev device using magnet array. **d** The distribution of the gradient magnetic flux intensity of standard MagLev device using single square magnets. **e** Correction of magnetic field of magnet array. Reproduced with permission from Ref. [9]. Copyright 2021 Elsevier

In this series of analysis, the design of the device ensures the linear relationship between the levitation height and the density. The device uses magnet arrays should be the same as the device constructed with integrated magnets. However, there is a minute difference of $B_z \frac{\partial B_z}{\partial z}$ between the two devices. The chamfers on each small magnet may be the cause of the result. These structures lead to the uneven upper surface of the array, which surely affect the distribution of the magnetic field. Figure 6.19e exhibits the calculation of the magnetic flux intensity along the centerline, by which the minute difference can be revealed. The experiments on standard density glass beads verify the accuracy of the device, as shown in Fig. 6.20.

As expected, the levitation heights were proportional to the density of the beads. The levitation results shows good agreement with the simulation results. For comparison, same experiments were carried out in device using the integrated magnets. The slight difference mentioned above can be observed in these experiments: the levitation of the same bead has a little difference between the two devices. Furthermore, the levitations using different media suggests similar results that the levitation height linearly relates to the density. Concluded from the experiments, the following points can be drawn: (i) the two devices have similar levitation abilities, which indicates the device using magnet arrays can afford the density measurement as well as the device using square magnets; (ii) the simulation can well reveal the $B_z \frac{\partial B_z}{\partial z}$ along the centerline, which could provide an accurate calculation method for density measurement with devices using different magnet arrays.

Take steps along the idea, a magnified MagLev device is constructed. The magnet array consists of 9 identical magnets with the arrangement of 3 * 3 * 1. The size of the magnet is 50 * 50 * 50 mm. To adjust the different occasions, the distance between the magnet arrays can be changed by a ball screw. As predicted, the repulsive force causes difficulties in arranging the magnet. Therefore, bolts are used to fix the magnets on the iron base board. But this brings another problem that the through-hole may greatly changes the magnetic field of the magnet. Fortunately, this structure of the magnet only has obvious effect near its surface, but will not significantly affect the higher area. In addition, magnify the device will also result in a reduction of

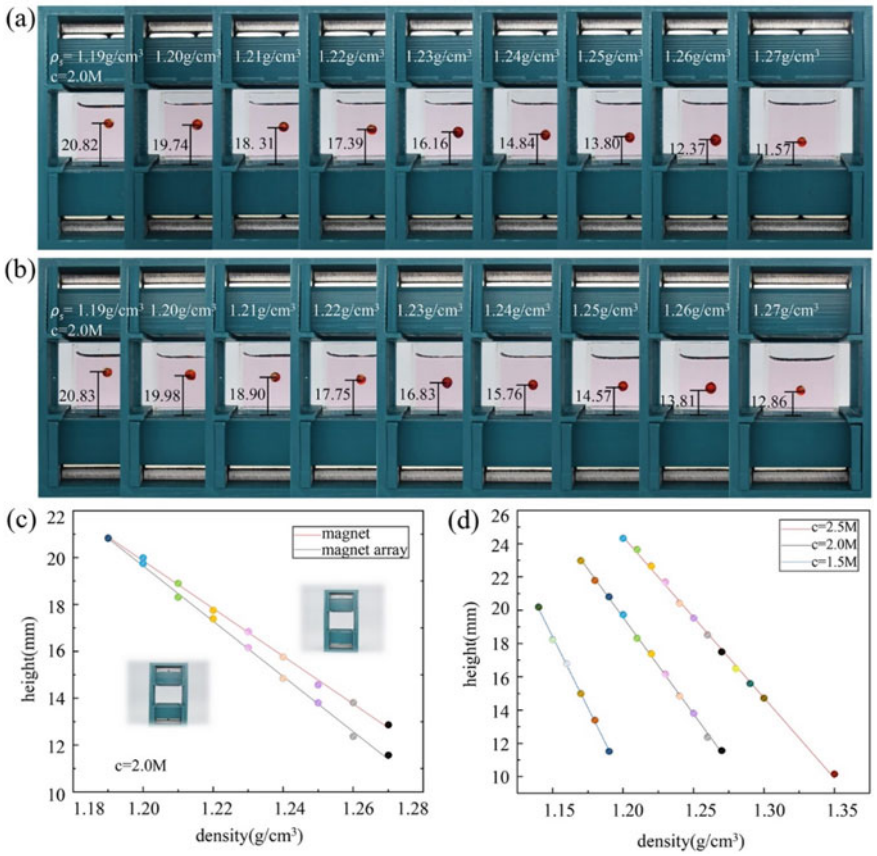

Fig. 6.20 Feasibility verification experiments using standard density beads. **a** Results obtained with the magnet array. **b** Results obtained with the square magnets. **c** Comparison of the results obtained from different devices. **d** Measurement results using media with different concentrations. Reproduced with permission from Ref. [9]. Copyright 2021 Elsevier

measurement range and enhance the sensitivity of the device. This is because the magnify of the magnet ensures the same surface magnetic flux intensity. However, the magnify of the device makes the distance of the magnets times larger than the standard MagLev device. While the larger distance causes less gradient of magnetic field. Finally, according to Eq. 5.7, the device cannot levitate denser materials as the standard MagLev device can, but will be sensitive to the minute density differences.

The above discussion can all be revealed in the experiments on standard density beads. As shown in Fig. 6.21, the measurement range is obviously smaller than the standard MagLev device. The difference of 0.01 g/cm^3 leads to a much larger difference in levitation height using the same medium. For instance, the levitation height intercept between 1.26 and 1.25 g/cm^3 in 2.5 M $MnCl_2$ aqueous solution is

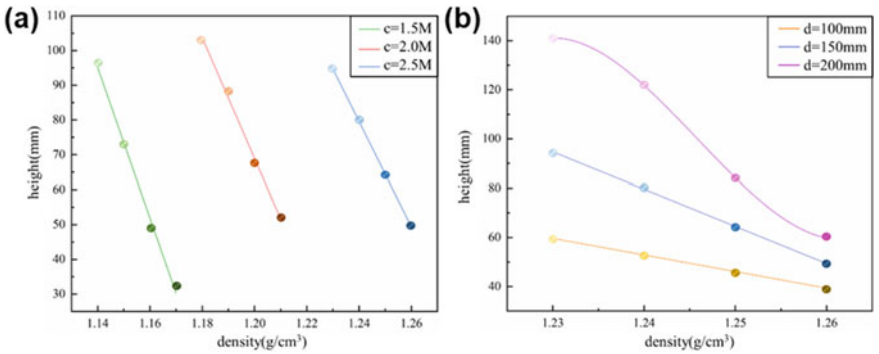

Fig. 6.21 Density measurement results using magnified MagLev device. **a** Measurement results using media with different concentrations. **b** Measurement results under different distance between the magnet arrays

2.6 mm using standard MagLev device. It comes to 24.42 mm when using magnet array device.

The high sensitivity and large operation area guarantee the detection of large objects. For instance, a trial on measuring carbon fiber reinforced polymer tensile bar is shown in Fig. 6.22. The bar has the width of 76 mm, which is definitely impossible for standard MagLev device to test. The density of the bar is measured as 1.502 g/cm^3. Compared with the results from common method (nominal density of 1.501 g/cm^3), the result has a high accuracy.

The most advantageous character of the device is the ability to test large polymer parts. For standard MagLev device, the maximum diameter of the part is restricted to 30 mm, not to mention the thickness should be much smaller (several millimeters). Moreover, the less sensitivity of the standard MagLev device cannot measure the density of thick parts precisely. This is also a disturbance in testing tiny defects of the part. While, these problems are all fixed in MagLev device with magnet array. A typical sample is the detection of the polyetherimide (PEI) base of aerospace craft

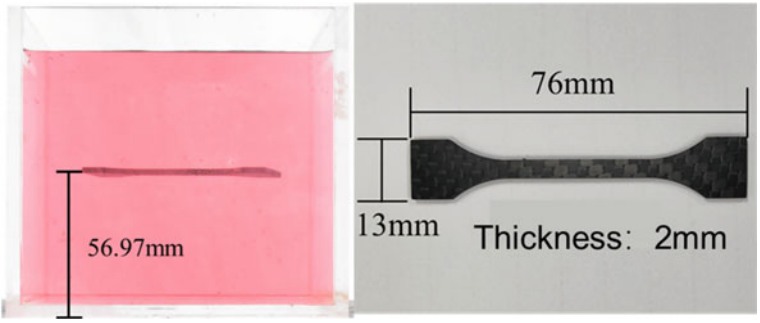

Fig. 6.22 Levitation of carbon fiber reinforced polymer tensile bar

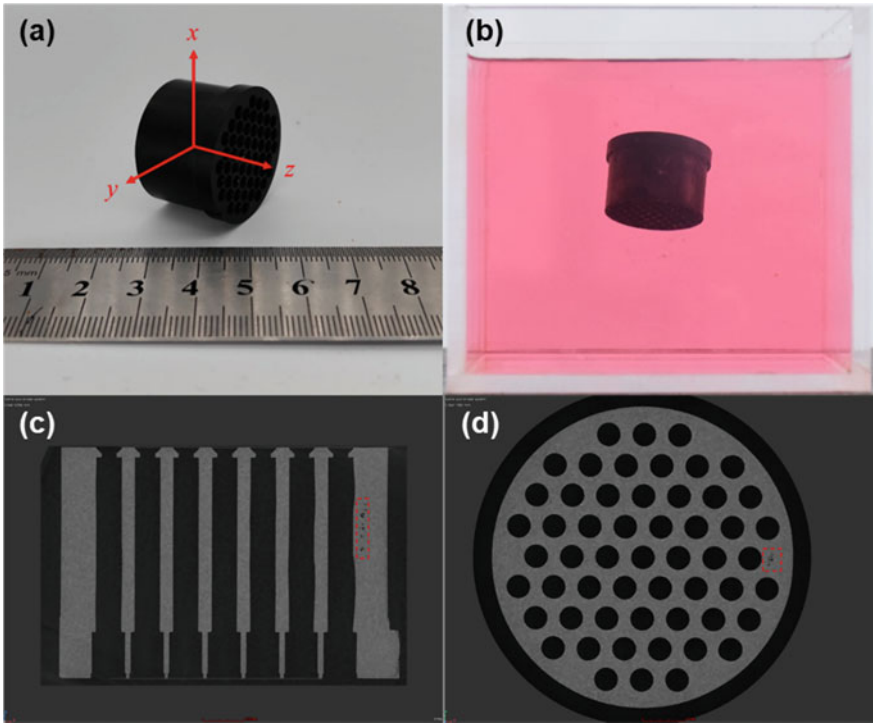

Fig. 6.23 Defect detection of PEI base of aerospace craft electric coupler. **a** Scale of the coupler. **b** Levitation result. **c**, **d** SEM test of the coupler

electric coupler, as shown in Fig. 6.23. The tilted levitation posture indicates the part has interior voids on upper direction. The SEM test verifies the MagLev testing result (Fig. 6.23c, d). Slight voids locates at the relatively thicker structure of the part, which cause an obvious incline of the part during levitation.

In general, although difficulties and disadvantages still occur along with predominant advantages of large operation area, higher sensitivity, and high accuracy, the magnify of the MagLev device by using magnet array is a promising for MagLev testing method to deal with large and complex parts with the mean density in the range from 0.8 to 2.0 g/cm^3.

6.4.3 Using Bar Magnets

The magnetic levitation can also be achieved by the bar magnets. A high throughput configuration was carried out by utilizing a re-engineered device based on bar magnets (Fig. 6.24a). The long levitation area is divided into several wells to separately handle very small amount of target materials in each wells. In practice, the

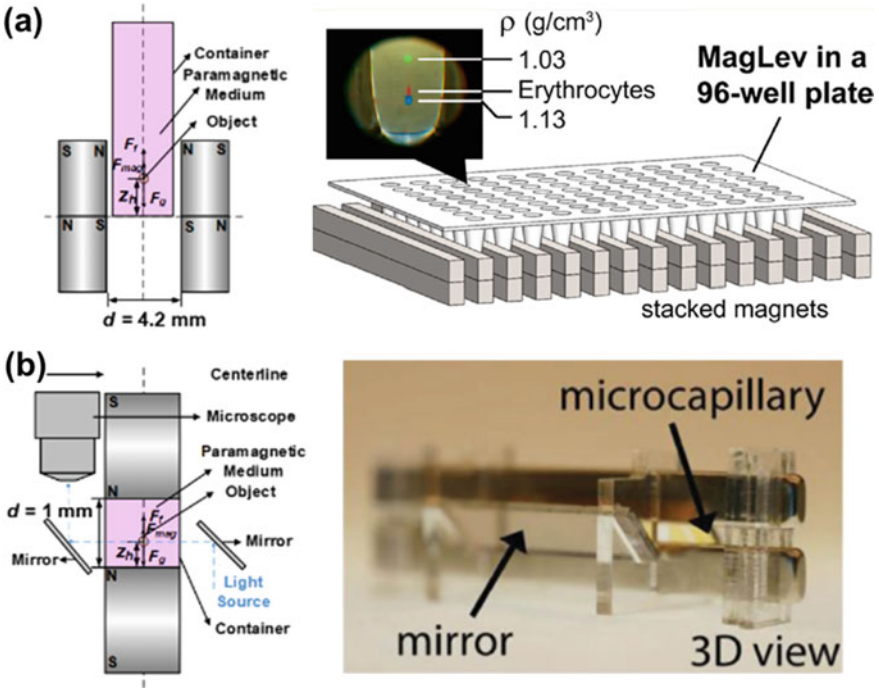

Fig. 6.24 MagLev using bar magnets. **a** High throughput configuration. **b** Configuration combines magnetic focusing and florescence microscopy. Reproduced with permission from the article "Current state of magnetic levitation and its applications in polymers: A review." Copyright 2021 Elsevier

device could measure 96 wells at the same time and still have potential to handle more wells. This configuration has promising applications in the field of materials chemistry, forensic evidence and analytical science.

Different from the levitation by square magnets, the MagLev device with bar magnets can also generate a long area between the magnets, which can concentrate small particles on a line. Combined with microfluidics, it opens up a novel direction in the application of MagLev in biology and medicine. This configuration combines magnetic focusing and florescence microscopy (Fig. 6.24b). The magnetic field would drive the particles to a line where the forces acting on the particle reaches a balance when they are passing through the channel between the two magnets in paramagnetic medium. For instance, polymeric microspheres (5–10 μm) could be concentrated and measured via the improved MagLev device within 120 s [10]. Considering the detectable size of the particle, it is especially suitable for focusing and detecting micro scale particles, such as polymer microspheres and cells [11–13]. Benefit from the stable levitation and concentration of cells inside the device, the self assembled 3D cell cultures [14] and weightlessness culture of mesenchymal stem cells [15] can be easily achieved. Noticing the device occupies much less space

than standard MagLev device and the operation space is relatively narrow, the smart phone can be employed to enhanced its ability of real-time monitoring, sorting and digital quantification of particles [10, 16–18].

Among the applications using this configuration, the detection of sickle cell is a typical case of successful application of the device. It indicates that the configuration could become a useful point of care diagnosis tool. Followed by the change of ion permeability, the shape of red blood cell become a sickle. The average density of red blood cells also increased with these changes. Finally, the red blood cells lose their function and finally result in the sickle cell disease (Fig. 6.25a). Cells through the tube between the two bar magnets could be focused and separated. The density differences between normal and sickle red blood cells could cause the deviation between their levitation heights (Fig. 6.25a). Additionally, it also can be noticed that the density distribution of normal red blood cells is uniform, while sickle red blood cells have a wide density distribution. These phenomena can be used to the rapid screening diagnosis of sickle cell disease. Benefit from the portability of MagLev device, handheld magnetic platform was developed for convenient and low cost self-testing [18–21].

This improved MagLev device was also successfully applied in the detection of cell membrane-bound and antigen–antibody bindings [22]. Ligand-coated microbeads can capture soluble antigens or bind to the antigens on the surface of the cell. The bindings would result in a density change on the beads and cause a physical aggregation of two types of particles, (Fig. 6.25b) which enables the detection of the bindings and enumeration for quantification. Another work proposed a magnetic susceptibility-based method to detect protein [23]. The target protein could be captured by a polymer microsphere. Another magnetic nanoparticle was then attached onto the captured protein. Thus, the polymer microspheres attached

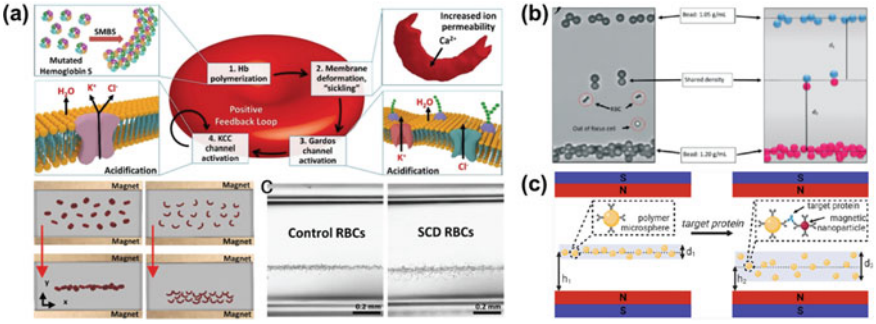

Fig. 6.25 Bio-applications of MagLev using bar magnets. **a** Diagnosis of sickle cell disease. **b** Detection of ligand-coated microbeads capture or bind to the antigens. **c** Detection of polymer microspheres attached with target protein and magnetic nanoparticles. Reproduced with permission from the article "Current state of magnetic levitation and its applications in polymers: A review." Copyright 2021 Elsevier

with target protein and magnetic nanoparticles would have different magnetic susceptibilities compared with those without protein, which finally reflects in the different levitation heights of the microspheres (Fig. 6.25c).

References

1. Nemiroski A, Soh S, Kwok SW, et al. Tilted magnetic levitation enables measurement of the complete range of densities of materials with low magnetic permeability. J Am Chem Soc. 2016;138(4):1252–7.
2. Xie J, Zhao P, Zhang C, et al. A feasible, portable and convenient density measurement method for minerals via magnetic levitation. Measurement. 2019;136:564–72.
3. Xie J, Zhang C, Gu F, et al. An accurate and versatile density measurement device: magnetic levitation. Sens Actuators B Chem. 2019;295:204–14.
4. Xie J, Zhao P, Jing Z, et al. Research on the sensitivity of magnetic levitation (MagLev) devices. J Magn Magn Mater. 2018;468:100–4.
5. Gao QH, Li WB, Zou HX, et al. A centrifugal magnetic levitation approach for high-reliability density measurement. Sens Actuators B Chem. 2019;287:64–70.
6. Ge S, Whitesides GM. "Axial" magnetic levitation using ring magnets enables simple density-based analysis, separation, and manipulation. Anal Chem. 2018;90(20):12239–45.
7. Zhang C, Zhao P, Gu F, et al. Axial-circular magnetic levitation: a three-dimensional density measurement and manipulation approach. Anal Chem. 2020;92(10):6925–31.
8. Zhang C, Zhao P, Tang D, et al. Axial magnetic levitation: a high-sensitive and maneuverable density-based analysis device. Sens Actuators B Chem. 2020;304: 127362.
9. Zhao P, Jia Y, Xie J, et al. Magnetic levitation for polymer testing using magnet array. Polym Testing. 2021;103: 107361.
10. Knowlton S, Yu CH, Jain N, et al. Smart-phone based magnetic levitation for measuring densities. PLoS ONE. 2015;10(8): e0134400.
11. Ge S, Wang Y, Deshler NJ, et al. High-throughput density measurement using magnetic levitation. J Am Chem Soc. 2018;140(24):7510–8.
12. Durmus NG, Tekin HC, Guven S, et al. Magnetic levitation of single cells. Proc Natl Acad Sci. 2015;112(28):3661–8.
13. Tasoglu S, Khoory JA, Tekin HC, et al. Levitational image cytometry with temporal resolution. Adv Mater. 2015;27(26):3901–8.
14. Anil-Inevi M, Yaman S, Yildiz AA, et al. Biofabrication of in situ self assembled 3D cell cultures in a weightlessness environment generated using magnetic levitation. Sci Rep. 2018;8(1):7239.
15. Anil-Inevi M, Yilmaz E, Sarigil O, et al. Single cell densitometry and weightlessness culture of mesenchymal stem cells using magnetic levitation. Stem Cell Nanotechnol Methods Protocols. 2020:15–25.
16. Amin R, Knowlton S, Yenilmez B, et al. Smart-phone attachable, flow-assisted magnetic focusing device. RSC Adv. 2016;6(96):93922–31.
17. Knowlton SM, Sencan I, Aytar Y, et al. Sickle cell detection using a smartphone. Sci Rep. 2015;5(1):15022.
18. Knowlton S, Joshi A, Syrrist P, et al. 3D-printed smartphone-based point of care tool for fluorescence-and magnetophoresis-based cytometry. Lab Chip. 2017;17(16):2839–51.
19. Yenilmez B, Knowlton S, Tasoglu S. Self-contained handheld magnetic platform for point of care cytometry in biological samples. Adv Mater Technol. 2016;1(9):1600144.
20. Yenilmez B, Knowlton S, Yu CH, et al. Label-free sickle cell disease diagnosis using a low-cost, handheld platform. Adv Mater Technol. 2016;1(5):1600100.
21. Subramaniam AB, Gonidec M, Shapiro ND, et al. Metal-amplified density assays (MADAs), including a density-linked immunosorbent assay (DeLISA). Lab Chip. 2015;15(4):1009–22.

22. Andersen MS, Howard E, Lu S, et al. Detection of membrane-bound and soluble antigens by magnetic levitation. Lab Chip. 2017;17(20):3462–73.
23. Yaman S, Tekin HC. Magnetic susceptibility-based protein detection using magnetic levitation. Anal Chem. 2020;92(18):12556–63.